J Nondestruct Eval (2016) 35:13
DOI 10.1007/s10921-015-0330-8

# On-Line Monitoring of Environment-Assisted Cracking in Nuclear Piping Using Array Probe Direct Current Potential Drop

**J. Y. Yoon[1] · Y. Kim[1] · S. Choi[1] · W. C. Nam[1] · I. S. Hwang[1] · L. Bromberg[2] · P. W. Stahle[2] · R. G. Ballinger[2]**

Received: 8 September 2015 / Accepted: 15 December 2015 / Published online: 29 December 2015


**Abstract** A direct current potential drop method utilizing array probes with measurement ends maintaining an equalized potential designated as equi-potential switching array probe direct current potential drop (ESAP-DCPD) technique has been developed earlier at Seoul National University. This paper validates ESAP-DCPD technique by showing consistency among experimental measurements, analytical solution and numerical predictions using finite element analysis (FEA) of electric field changes with crack growth in metals. In order to examine its viability as an on-line monitoring of environment assisted crack growth at the inner surface of piping welds, artificial inner surface cracks were introduced in a full-scale weldment mockup pipe and stainless steel metal mockup pipe. The weldment was joined by low alloy steel and stainless steel pipes. The pipes were monitored by using ESAP-DCPD in laboratory environments. Optimization of electrical wiring configuration has produced results with significantly reduced noise for adequately long period of time. Then optimized experimental results were compared with the FEA prediction results for the mockup to show a good agreement. Also a round-robin measurement has been made at three laboratories. It has been found that the developed ESAP-DCPD can detect circumferential cracks with a depth of 40 % of wall thickness in stainless steel with a good detectability for further growth behaviors. For axial cracks, however, the measurements showed poor detectability. Hence the developed ESAP-DCPD system can be used to monitor large circumferential cracks that existing non-destructive examination techniques often fail to detect until leakage takes place.

**Keywords** Array probe · Direct current potential drop (DCPD) · Dissimilar metal weld · Finite element analysis (FEA) · Surface crack · Potential drop ratio

## Abbreviations

| | |
|---|---|
| CCT | Center cracked tension |
| CV | Coefficient of variation |
| DMW | Dissimilar metal weld |
| EDM | Electrical discharge machined |
| EAC | Environment-assisted cracking |
| ESAP-DCPD | Equi-potential switching array probe direct current potential drop |
| FEA | Finite element analysis |
| LAS | Low alloy steel |
| NDE | Non-destructive examination |
| NPLC | Number of power line cycles |
| OD | Outer diameter |
| UT | Ultrasonic testing |
| ECT | Eddy current testing |
| PDR | Potential drop ratio |
| PWR | Pressurized water reactor |
| PWSCC | Primary water stress corrosion cracking |
| RRT | Round-robin test |

## Roman Letters

| | |
|---|---|
| $a$ | Crack depth |
| $t$ | Pipe wall thickness |
| $V_l$ | Leak voltage |

✉ J. Y. Yoon
ssoryjy0@snu.ac.kr

[1] School of Energy System Engineering, Seoul National University, One Daehak-ro, Gwanak-gu, Seoul 151-744, Republic of Korea

[2] Department of Nuclear Science and Engineering, Massachusetts Institute of Technology, 77 Massachusetts Avenue, Cambridge, MA 02139-4307, USA

| | |
|---|---|
| $V_t$ | Target voltage |
| $V_r$ | Reference voltage |
| $g_1$ | Current lead wire spacing |
| $g_2$ | Probe wire spacing |

## 1 Introduction

Operating light water reactors have been designed for a 40 years life span in general. It has been shown that most nuclear power plants (NPPs) can be maintained to have adequate safety margin as well as economic incentives to run beyond their original design life. In the U.S., the life extension up to 60 years has been accepted for many operating NPPs. Recently, the life extension up to 80 years is being planned. The most important question to this effort is how to assure the plant safety against materials degradation modes in passive components including piping and pressure vessels. Although there exist well-established rules and standards for the inspection and maintenance of the passive components in accordance with ASME Boiler and Pressure Vessel Code, particularly Sec XI [1], limited but noticeable events have been caused by environment-assisted cracking (EAC) of welds, calling for more conservative measures, as shown in Fig. 1. Especially primary water stress corrosion cracking (PWSCC) in Pressurized Water Reactors (PWRs) has been blamed for several undetected cracks that exceed ASME Boiler Pressure Vessel Code criteria. Several PWSCC produced through-wall cracks within dissimilar metal welds (DMWs) at piping and penetration nozzles [2–5]. It is well known that conventional non-destructive examination (NDE) such as ultrasonic testing (UT) or eddy current testing (ECT) has limitations in detecting even large cracks in weldments.

Deep circumferential cracks are particularly important as they can lead to unstable crack growth upon earthquake loading on piping welds if they are left undetected in in-service inspection. The Fukushima accident has displayed the need for safety assessment considering beyond-design basis events such as earthquakes with greater accelerations. With increasing plant lives, such a beyond-design basis analysis should take into account the effect of EACs. It is conceivable that deep EACs left undetected may break nuclear piping under dynamic loading aggravating accident. On-line monitoring techniques can significantly enhance the probability of detection for large growing EACs [6].

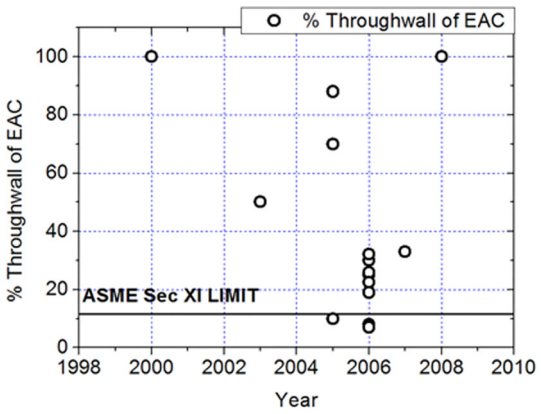


**Fig. 1** Crack indication detected in Alloy 82/182 butt welds of a reactor coolant loop [5]

In order to monitor EAC growth behavior in welds at NPPs and hence to prevent code violations, the viability of advanced inspection and monitoring techniques is needed. In this study, direct current potential drop (DCPD) technique is examined for its suitability for on-line monitoring of piping welds. The reliability of the conventional DCPD method has been widely demonstrated by extensive experiences at lab scale experiments [7,8]. In addition, there have been significant demonstrations by applying the converted DCPD to the nuclear power plant piping in Germany. Exploratory field experiences applying DCPD technique to operating nuclear power plant piping by TUV Rheinland, Germany, can be utilized in building the solid basis for further applications [9–12]. The German exploratory effect was, however, discontinued without any significant reports.

Ryu et al. installed the equi-potential switching DCPD technique to the secondary side piping elbow in Korean nuclear power plant to demonstrate that electric current can be confined within measurement areas without any safety concern [13]. The Equi-potential Switching Array Probe DCPD (ESAP-DCPD) which can eliminate any stray current outside of monitoring piping is improved from previous technique to detect surface cracks in nuclear piping by using an array of probes.

In this paper, the signal validity and reproducibility of ESAP-DCPD will be demonstrated in optimized conditions against both theoretical solutions and finite element analysis (FEA).

## 2 ESAP-DCPD Development

### 2.1 Description of ESAP-DCPD Method

The equi-potential switching array probe direct current potential drop (ESAP-DCPD) method has evolved from the existing switched DCPD technique which has been used in laboratories to measure crack size [14,15]. Switching current direction and subtracting measured signal pair are well established methods to eliminate the thermoelectric effect [16]. Array probes are also often used to measure potential distribution over an area of interest [17]. The Equi-potential technique has been developed earlier at the Seoul National University as an innovative technique to limit applied DC

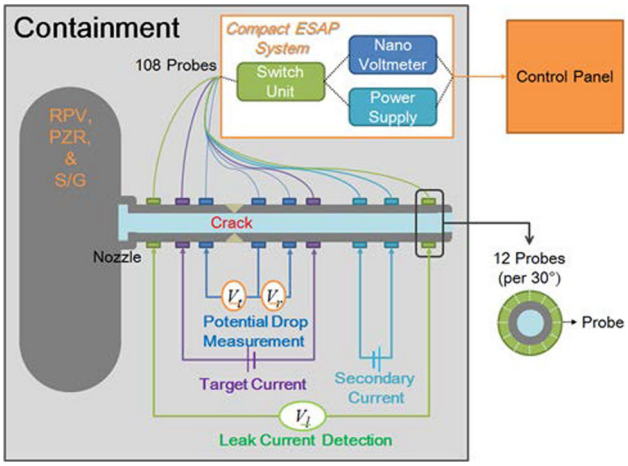


**Fig. 2** Schematic diagram of on-line monitoring of EAC in a weld region of a PWR reactor coolant piping using ESAP-DCPD system


**Fig. 3** Photograph of electronic components of ESAP-DCPD system

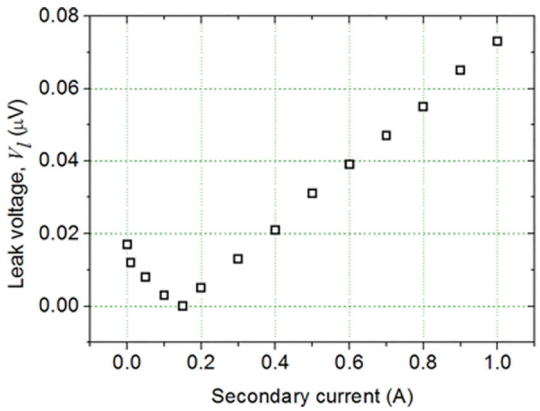


**Fig. 4** Potential drop cause by leakage current as a function of secondary current

flow to within a suspected area so that no potential disturbances can take place in any other regions [13,18,19]. ESAP-DCPD has been developed as a new technique for on-line monitoring of materials degradation by integrating these useful elements.

We focus on applying the method to monitor the defect in piping weldments. At this stage of development, the technique is not developed to substitute existing NDE techniques. Instead it is intended to complement periodic NDE campaigns. In contrast with periodic NDE, ESAP-DCPD has a significant advantage that it can be fixed to the specific weld area without disturbance, thus maximizing signal consistency. And it also can be used to monitor cracks in real time to identify data trends which can increase the probability of detection.

Schematic wiring diagram of the on-line monitoring method using ESAP-DCPD is shown in Fig. 2. There are nine sets of wire arrays over the measurement area of pipe; three sets are for potential measurements with two sets of direct current supply on the left side of piping in Fig. 2. The potential drop at the crack defined as target voltage, $V_t$, is measured with the potential drop at non-cracked location defined as reference voltage defined, $V_r$. Additional four sets on the right side are for auxiliary current supply and potential monitoring so that leak current can be eliminated. The potential drop for leak detection is defined as leak voltage, $V_l$. Each set consists of twelve wires that are distributed over the circumference with equal spacing, as described in Fig. 2.

The ESAP-DCPD hardware consists of two programmable power supplies, one nano-voltmeter, a current switching module and sets of twelve array probes. Figure 3 shows a photograph of ESAP-DCPD hardware. The first power supplier provides a switched direct current for crack detection and the secondary power supplier removes leak current by maintaining an equipotential loop. The equipotential loop eliminates any chance for introducing a spurious potential drop outside of the measurement area and hence no adverse effect is expected on existing sensors and instruments of the power plant. The elimination of the leak current is demonstrated in Fig. 4. When the primary current is 1A, the secondary current is automatically adjusted to 0.15A for minimizing the leakage current.

Switching module changes the current flow periodically to suppress the noise produced from thermoelectric effect. It was already confirmed that the noise level decreased when switching the direction of current flow [16]. It can also treat many potential drop signals for convenient data processing. Because the switching controller can only carry a small current, solid state relays with high current ratings are used for the primary current. The array probes measure the potential drop across the axis of the pipe and the data is acquired and transferred to a computer, where it can be analyzed. The probes are fixed on the pipe surface by using an inner spring and clamp to maintain good contact. As the system allows for on-line monitoring of the pipes, real-time data can be acquired.

Typical piping welds for the primary system of PWR are expected to use the main current not exceeding 30 A. The potential drop across the weld is in the range of several microvolts. Due to the high electric resistance of the primary coolant, no electrochemical effect is expected to aggravate corrosion characteristics.

In this study, the measured DCPD value is normalized by the reference signal. Then the change in the normalized signal with time is measured by the relative value as defined in Eq. (1). It is defined as potential drop ratio (PDR). The normalization by the reference potential is instrumental in taking into account the change of temperature or current intensity.

$$PDR(\%) = \left( \frac{V_t}{V_{t0}} / \frac{V_r}{V_{r0}} - 1 \right) \times 100 \quad (1)$$

where $V_t$ is target voltage, $V_{t0}$ is initial voltage (t = 0), $V_r$ is reference target voltage, and $V_{r0}$ is reference initial voltage (t = 0).

### 2.2 Validation of ESAP-DCPD Against Theoretical Solution and Finite Element Analysis (FEA)

There have been many studies about the prediction of DCPD behaviors using FEA. Some investigated the relationship between potential drop as a function of crack size by performing FEA [20,21]. The detectability of cracks in the pipe using DCPD was also predicted by FEA [22]. The optimal location of current lead wire was analyzed for compact tension specimen [23] and for a plate geometry [24]. Induced current potential drop technique was introduced for detecting an axial crack in a tube shaped specimen through FEA [25]. Pipe wall thickness was evaluated by using array probes DCPD through FEA [17]. DCPD behavior at the edge of plate was evaluated by comparing analytic solution with theoretical calculation and measurements [26,27]. Unlike those studies, this work has been focused on the validation of measured potential in the welded pipe against theoretical solution and numerical solution solved by FEA.

At the first step, the result of FEA was verified against a well-known analytical solution. Then a comparison has been made to show a good agreement among three important approaches: numerical solution, analytic solution and experimental measurement for the center cracked tension (CCT) specimen designed in accordance with ASTM E647 standard, as shown in Fig. 5 [28].

For the flexibility of the ESAP-DCPD measurement, the array probe wires were forced to make point contacts with CCT by using helical springs. Unlike piping networks, the CCT specimen is already electrically isolated with the lack of extending electric circuits and hence the secondary current was not used in this test. There are five sets of electric

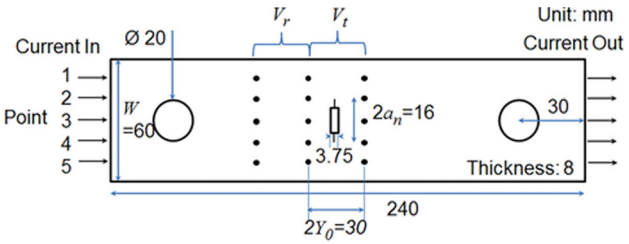


**Fig. 5** Design of center cracked tension (CCT) specimen

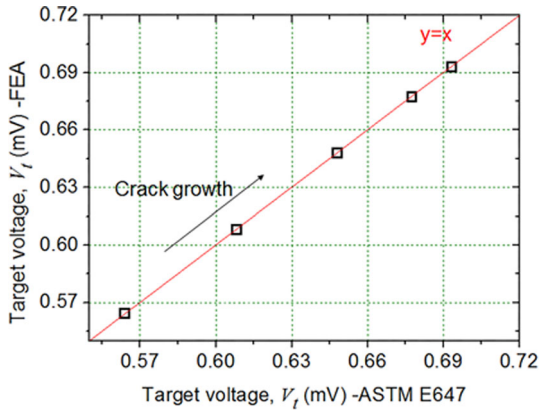


**Fig. 6** Comparison between finite element analysis (FEA) results and analytic solution from ASTM equation at point 3 on the CCT specimen

contacts including a pair of current lead wires and three sets of potential measurement array probes.

The electrical field analysis was performed by FEA for DC flow from one end of the specimen to the other. The electrical resistivity of Type 304 Stainless Steel as $7.2 \times 10^{-4} \Omega$ mm was used [29]. FEA was performed as a function of crack size. The analytic solution given in ASTM E647 has been employed as the theoretical solution, as shown in Eq. (2) [28]. FEA focuses on the DCPD across the center crack at the mid-plane intersecting point 3 horizontally in the specimen that Eq. (2) is derived for. Figure 6 shows a good agreement between FEA results and the analytic solution with only 0.05 % maximum error. ASTM only indicates the potential drop as target voltage without reference voltage at the center cracked region and hence only the target voltage was compared here.

$$a_n = \frac{W}{\pi} COS^{-1}\left[ \frac{COSH\left(\frac{\pi}{W} \times Y_0\right)}{COSH\left[ \frac{V}{V_0} \times COSH^{-1}\left[ \frac{COSH\left(\frac{\pi}{W} \times Y_0\right)}{COSH\left(\frac{\pi}{W} \times a_0\right)} \right] \right]} \right] \quad (2)$$

where $a_n$ is crack size (as defined in test method E647), $a_0$ is reference crack size from some other method, $W$ is specimen width, $V$ is measured voltage, $V_0$ is measured voltage corresponding to $a_0$, and $Y_0$ is voltage measurement lead spacing from the crack plane.

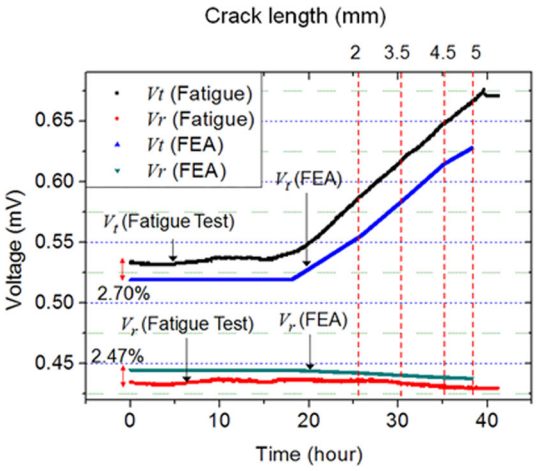


**Fig. 7** Measured target and reference voltage by fatigue test and FEA at point 4 on the CCT specimen

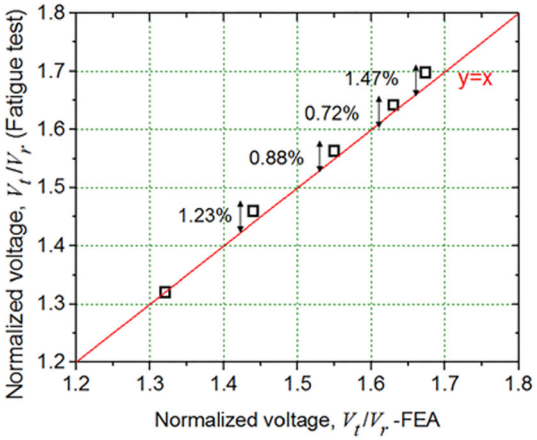


**Fig. 8** Comparison of normalized voltage between experimental measurement and FEA at point 3 on the CCT specimen

Subsequently, the fatigue crack growth test was done in air at room temperature using the CCT specimen made of Type 304 Stainless Steel. The mode of fatigue test was constant $\Delta K$ at 10 Hz with R ratio of 0.1. The fatigue crack growth was observed visually by using traveling microscope. Figure 7 shows the experimental results of DCPD and FEA results at point4 in the specimen where the crack growth initiated until crack length reached 5 mm. Both experimental and FEA results show the target voltage increases as crack grows whereas the reference potential almost remains constant with 2.5 % error. At the mid-plane intersecting point 3 in the specimen, the measured normalized voltage which is the ratio of target to reference agrees well with FEA results by about maximum 1.5 % error, as shown in Fig. 8. The normalized voltage was evaluated as an ultimate objective, in here, in order to eliminate the temperature changing effect and the current fluctuation of power supplier. The reason why the error occurs is that there are a current lead wire resistance and a potential measurement probe wire resistance in the experiment unlike FEA and analytic solution. In summary, the comparison between measured data and FEA shows a good agreement. They also agree well with Eq. (2).

### 2.3 Optimization of ESAP-DCPD System

The components of ESAP-DCPD were introduced in previous section. In addition to those instruments, sets of array probes are very significant components affecting the detection of cracks. Especially arrangement of probes is critical factor to obtain high probability of detection for circumferential crack. The probe consists of sharp tip made of brass, body made of aluminum and Banana plug for wiring works. The array probes installed at the outer surface of the pipe were pressed to make point contacts using helical springs. In this study, two factors were analyzed for the dissimilar metal weld pipe for evaluating the detectability of crack, as described in Fig. 9; the spacing of current lead wire probes and the number of probes. The circumferential semi-elliptical crack was located at the 30° angle of pipe inner surface from the centerline of DMWs pipe between Type304 stainless steel and A508 low alloy steel (LAS) of a pressurizer surge line nozzle in PWRs. Total 10 ampere of current was passed through the pipe weld measurement region. Table 1 shows the input data of FEA for DCPD prediction at the pipe weld region.

Figure 10 shows the finite element model of a surface inner crack using tetrahedral coupled field solid element for electric analysis. In order to determine optimal configurations of probe and current lead wires, a series of FEA was conducted on the pipe weld geometry with current lead wire spacing ($g_1$) and probe wire spacing ($g_2$) as variables. The probe wire spacing, g2 was fixed as 5cm, so that weldment which is monitoring target could be located between two probe wires. Past study showed that as the separation between current lead wires decreases, the potential drop may increase for a fixed probe wires spacing [24]. However ESAP-DCPD

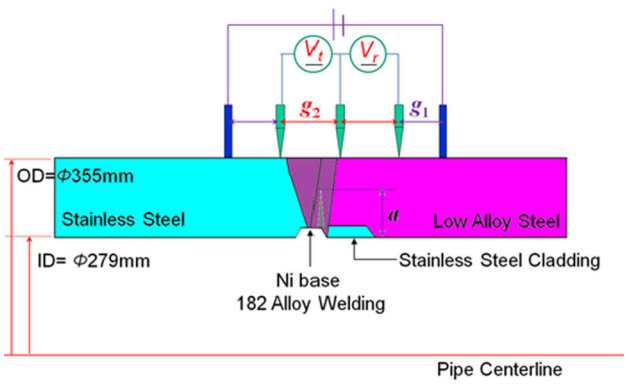


**Fig. 9** Schematic design of simulated dissimilar metal weld pipe mockup

**Table 1** Input for finite element analysis of dissimilar metal welds for mockup pipe of Type 304 stainless steel and A508 low alloy steel

| Input parameter for FEA | |
|---|---|
| Material (Base metal1) | Type 304 stainless steel |
| Material (Base metal2) | A508 low alloy steel (LAS) |
| Material (Weldment) | Alloy 182 Ni base |
| Pipe outer diameter (mm) | 355 |
| Pipe inner diameter (mm) | 279 |
| Pipe thickness (mm) | 38.0 |
| Length of stainless steel | |
| In outer surface of the pipe (mm) | 287 |
| Length of low alloy steel | |
| In outer surface of the pipe (mm) | 279 |
| Length of weldment | |
| In outer surface of the pipe (mm) | 45.2 |
| Cladding thickness (mm) | 5.08 |
| Electric resistivity of Type304 (Ω mm) | $7.20 \times 10^{-4}$ |
| Electric resistivity of A508 LAS (Ω mm) | $1.03 \times 10^{-3}$ |
| Electric resistivity of Alloy 182 Ni base Weldment (Ω mm) | $1.71 \times 10^{-4}$ |

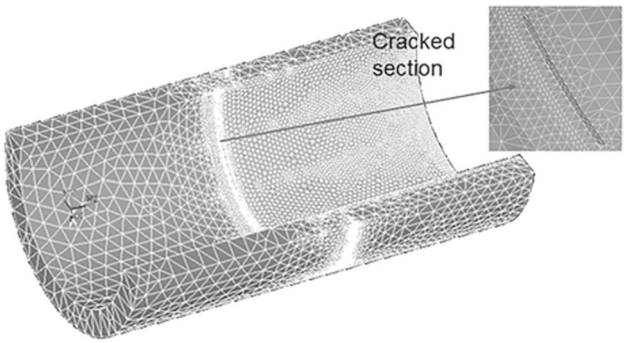


**Fig. 10** Meshed structure of inner surface crack at the weldment in the pipe mockup

**Table 2** Standard deviation of potential drop ratio at all angles with variable current lead wire spacing ($g_1$) when the pipe is pristine state

| Current lead wire spacing, $g_1$ (cm) | 3 | 5 | 7 | 10 | 15 |
|---|---|---|---|---|---|
| Standard deviation (%) | 17.6 | 4.01 | 2.32 | 0.686 | 1.91 |

uses two pairs of current lead wires for main current input and for current leakage minimization, respectively, which make a distinction from those used in past studies. Spacing between current lead wires is made large enough to avoid signal disturbances.

Furthermore, it is desired to allow enough current lead wire spacing for uniform current flow all around the circumference in the weld region. The effect of current lead wire is demonstrated by FEA as shown in Fig. 11a. Both target potential drop ($V_t$) and reference potential drop ($V_r$) increase with decreasing current lead wire spacing as anticipated. However, PDR decreases with decreasing current lead wire spacing because the increasing rate of target potential drop is smaller than that of reference potential drop. For optimal current lead wire spacing, 10 cm instead of 15 cm was selected due to two reasons. First, DCPD is most stable with 10 cm current lead wire spacing by performing additional FEA with non-cracked pristine state of pipe. It is expected that PDR is same at all angles which means the variance of the PDR at all angles equals to zero. Table 2 shows the standard deviation of 10 cm current lead wire spacing is smaller than the other cases. Second, 10 cm current lead wire spacing enables PDR to increase more rapidly than 15 cm current lead wire spacing when a crack propagates. The increase rate of PDR with crack growth is important because DCPD is suitable for on-line monitoring of crack growth.

Then FEA was extended to determine optimal configuration of array probes with a fixed distance between current lead wires. Figure 11b shows that the more probes are used, the higher PDR is obtained. However, the optimal number of probes for one set was determined to be 12 over the cir-

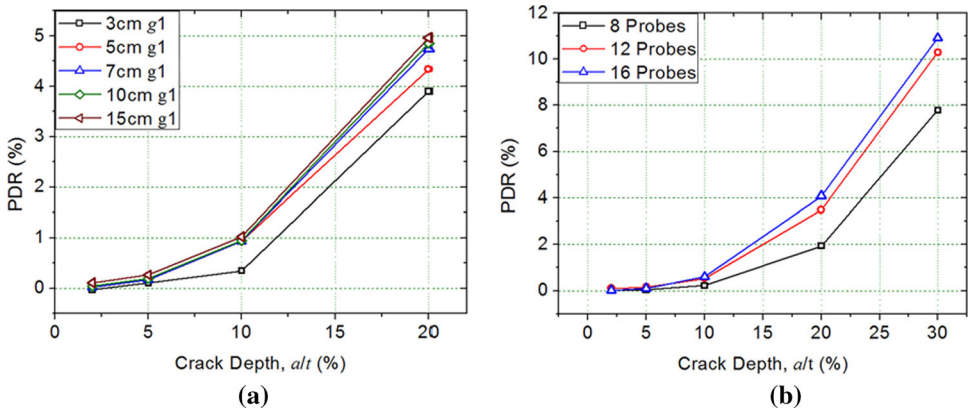


**Fig. 11** Simulated potential drop ratio (PDR) **a** with various current lead wire spacing (g1) and **b** with various number of probes for the pipe weld mockup as predicted by FEA

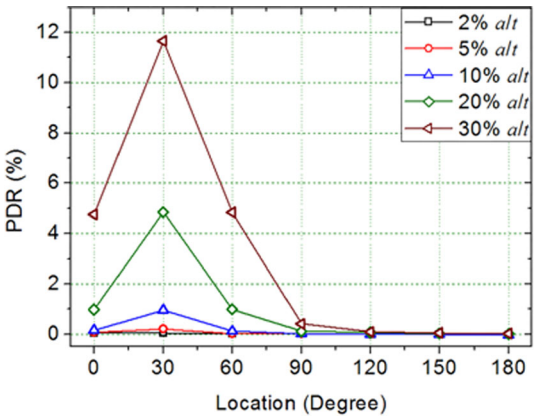


**Fig. 12** Simulated PDR with various crack depth for the pipe weld mockup as predicted by FEA

cumference of pipe weld, so that total number of five sets of measuring probes cannot be over 60. In order to measure 60 probes, 36 channels are needed; 24 channels for three sets of probes, 12 channels for two sets of probes. If total number of measuring probes is over 60, one more switching module is needed because one switching module can include two multiplexers which are possible to handle 40 channels.

By using the optimal configurations of array probes and current lead wires distance, FEA was conducted to investigate the detectability of environment-assisted crack at the inner surface. If the PDR is higher than 0.5 % which is three times standard deviation of signal, it is judged that a crack is detected. Figure 12 shows the method can detect 10 % a/t crack, well suitable to detect severe cracks. Because maximum acceptable crack depth is 10.9 % of a/t as explained in the section of IWB-3500 managing the acceptance standards in the division 1 of ASME Boiler and Pressure Vessel Code Section XI [1].

Additionally, measurement condition was optimized to minimize noise and drift of voltage signals through sensitivity study. The current lead wires were stabilized by clamping surface contact with pipe outer wall. At the beginning of a new measurement, the ESAP-DCPD electron system was turned on with the warming up time for 30 min with a live current to ensure stability of DC power supplier. A large and whole number of power line cycles (NPLC) were used to reduce noise from power line. Also the short delay time was inserted between each measurement to minimize data logging errors. Optimum NPLC and delay time, respectively, were determined as 20 and 15 s from the sensitivity study results as described in Table 3. The coefficient of variation (CV) which is well known as relative standard deviation in statistics is used to evaluate the noise level. It is explained in Eq. (3). The data processing was improved by introducing the moving average method after rejecting outlying data exceeding three standard deviations. When the current switching

**Table 3** Coefficient of variation (%) as a function of averaging number of power line cycles and delay time obtained from sensitivity study

| NPLC | Delay time | | | |
|---|---|---|---|---|
| | 5 | 10 | 15 | 20 |
| 1 | 0.336 | 0.255 | 0.0995 | 0.116 |
| 20 | | | 0.0326 | |
| 100 | | | 0.0431 | |
| 150 | | | 0.0353 | |
| 200 | | | 0.0951 | |

occurred after all channels at array probes were measured successively, the waiting time for 10minutes was inserted for a stabilization of signals.

$$CV = \sum_{i=1}^{n} \left(\frac{\sigma}{\mu}\right)_i \Big/ n \tag{3}$$

where $\sigma$ is the standard deviation of signal at each angle, $\mu$ is the mean of signal at each angle, and n is the number of angles.

## 3 Experimental and Discussions

### 3.1 Experimental

In order to estimate the detectability of cracks using ESAP-DCPD, real size pipe containing artificial cracks was monitored in real time and the results were compared with FEA. The outer diameter (OD) of the pipe is 355 mm with a 37 mm thickness with variance and the length of pipe is 611 mm. The pipe rented from Korea Plant Service & Engineering Co., Ltd. included four circumferential inner surface cracks at DMWs made of Alloy 182 joined between stainless and carbon steel as described in Table 4. The geometry of pipe weld is same with the one used in FEA as describe in Fig. 9.

The applied current is 10 A and secondary current is automatically adjusted to about 1.5 A. The applied current is ten times of the optimal current condition and it is expected to further increase the signal to noise ratio [16]. Figure 13 shows that a signal noise level exceeding 0.36 % of CV was obtained without using optimal measurement conditions explained in Sect. 2.3 because optimal measurement conditions were not established at that time. Figure 13 shows that the highest normalized voltage was obtained at the 240° angle and the 330° angle though the largest crack with a depth of 20 % of wall thickness was located at the 219.9° angle. If ESAP-DCPD had a good detectability for the crack with a depth of 20 % of wall thickness, the normalized voltage at the 210° angle would be highest. However, the normalized voltage

**Table 4** Geometry of inner surface flaws in real size dissimilar metal weld pipe mockup

| Flaw no. | Orientation | Length (mm) | Depth (a/t, %) | Flaw Centerline Deg | Pipe thickness (mm) |
|---|---|---|---|---|---|
| 1 | CIRC | 9.83 | 7.3 | 24.90 | 36.9 |
| 2 | CIRC | 12.6 | 10.9 | 129.80 | 37.8 |
| 3 | CIRC | 18.9 | 19.6 | 219.90 | 36.6 |
| 4 | CIRC | 13.1 | 10.4 | 289.90 | 37.4 |

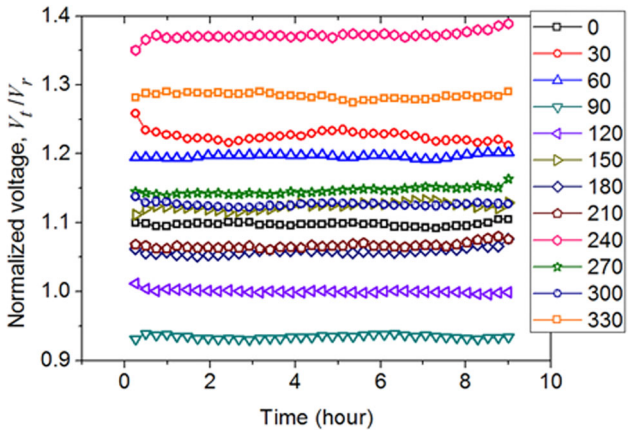


**Fig. 13** Measured normalized voltage of real size dissimilar metal weld pipe mockup through on-line monitoring

**Table 5** Geometry of flaws in stainless steel pipe mockup

| Flaw no. | Orientation | Length (mm) | Depth (a/t, %) | Flaw Centerline Deg |
|---|---|---|---|---|
| 1 | CIRC | 21.6 | 20 | 0 |
| 2 | CIRC | 32.4 | 30 | 90 |
| 3 | CIRC | 43.2 | 40 | 180 |
| 4 | CIRC | 54.6 | 50 | 270 |

at the 210° angle described by brown pentagonal shape is ninth highest against expectation. In other words, it is concluded that ESAP-DCPD is difficult to detect the crack with a depth less than 20 % of the wall thickness in welded pipe. Furthermore, DCPD in welded pipe is significantly affected by pristine state of pipe due to non-uniform distribution of weldment over the circumference. However, there is no information about pristine state of the pipe. Therefore, instead of welded pipe, stainless steel pipe without weldments which is less affected by pristine state was prepared. It included four circumferential electrical discharge machined (EDM) notches with a depth over 20 % of wall thickness, as shown in Table 5. The OD of pipe is 165.2 mm with a 18.2 mm thickness and the length of pipe is 450 mm. Figure 14 shows the installation of array probes on stainless steel pipe. Figure 15 shows the monitoring results of normalized voltage with 0.07 % CV which is reduced from 0.36 % by using optimized measurement conditions. The results show the normalized

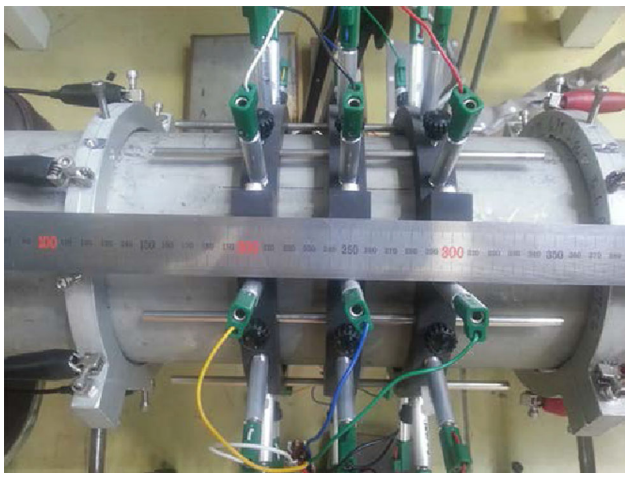

**Fig. 14** The photograph of installation of array probes on stainless steel pipe mockup

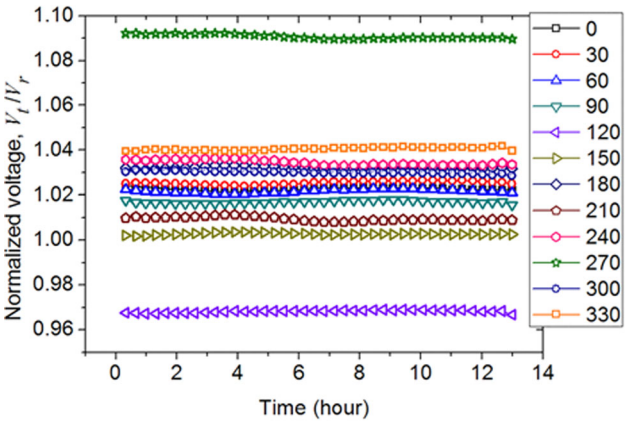


**Fig. 15** Measured normalized voltage of stainless steel pipe mockup using optimal conditions through on-line monitoring

voltage at the 270° angle described by green star is higher than the other data evidently as anticipated, and hence it was confirmed that the notch with a depth of 50 % of wall thickness could be detected by using ESAP-DCPD. In order to evaluate the detectability of notch at the other angles, measured results were compared with FEA as described in Fig. 16. The results, showing an agreement with 1.94 % error between measurement and FEA, give an evidence that the notch with a depth over 40 % of wall thickness could be detected by using ESAP-DCPD. The normalized voltage at

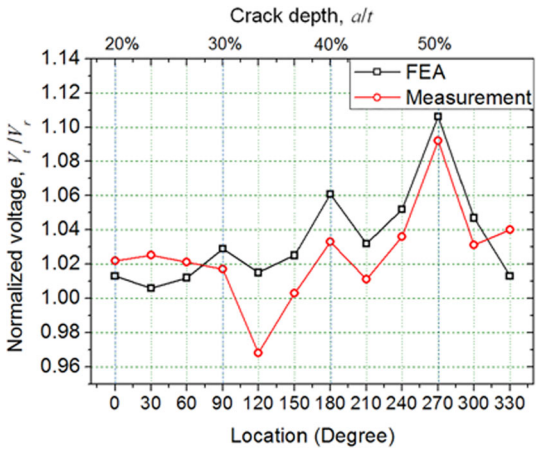


**Fig. 16** Comparison of normalized voltage between measurement and FEA by using stainless steel pipe mockup containing four circumferential notches

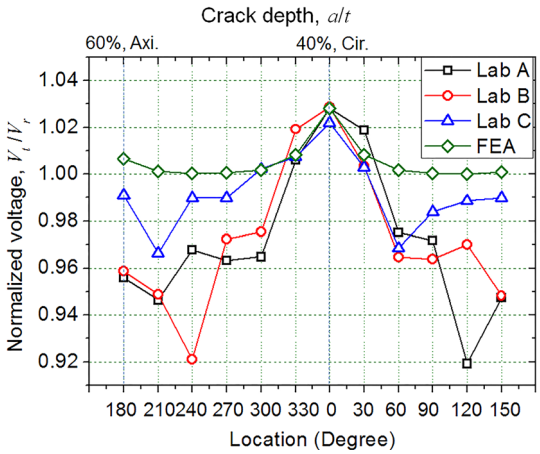


**Fig. 17** Measured normalized voltage obtained from round-robin test results at three laboratories for the stainless steel pipe mockup

the 40 % crack is 2.6 % higher than the normalized voltage at points of both sides with same tendency of FEA results. The normalized voltage at the 50 % crack is 5.7 % higher than the normalized voltage at points of both sides. It has been verified using stainless steel pipe and its verification with a welded pipe will be introduced in the near future.

### 3.2 Round Robin Test

In order to verify the reproducibility of ESAP-DCPD, round-robin test (RRT) was performed at three laboratories by using a stainless steel pipe produced for RRT. The pipe included one circumferential EDM notch with a depth of 40 % of wall thickness at the 0° angle and one axial EDM notch with a depth of 60 % of wall thickness at the 180° angle. Through RRT, it was proved that ESAP-DCPD has a reproducibility with good detectability for a circumferential notch with a depth of 40 % of wall thickness whereas it does not have detectability for axial notch, as demonstrated in Fig. 17. The problem is that measured normalized voltage at the other angles except the 0° angle is lower than 1 due to electrical noise. It remains as a future work to be resolved.

### 3.3 Discussions

The ESAP-DCPD has been developed for on-line monitoring of circumferential cracks of pipe welds that are vulnerable to environment assisted cracking. It is important to monitor circumferential cracks because dynamic load under earthquakes can lead to double-ended guillotine break which becomes an important issue after the Fukushima accident. It was shown that circumferential cracks with a 40 % depth a/t from the inner surface can be detected by using ESAP-DCPD instrumented on the outer surfaces of the pipe weld.

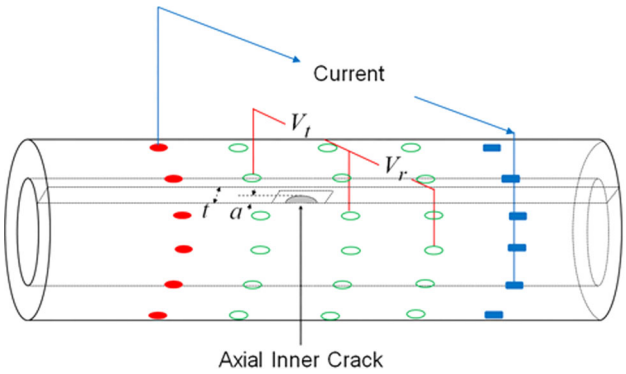


**Fig. 18** Schematic diagram of ESAP-DCPD for detection of axial crack in the stainless steel pipe mockup

In this paper, however, it is attempted to detect the axial cracks since detection of axial cracks is also needed to confirm safety of nuclear power plant piping. Figure 18 shows a schematic diagram of how to detect the axial crack on inner surface of the pipe which is simulated through FEA. Tilted current with the 30° angle to the pipe axis was sent diagonally from the one input point to the one output point. The scheme of diagonal current flow was repeated twelve times by moving the input point from one current lead wire to another one along the circumference. The pipe was measured by DCPD along the path tilted to the pipe axis with the 30° angle in order to monitor the axial crack. Figure 19 shows the FEA results for detection of axial crack (a) by using horizontal current method with existing ESAP-DCPD (b) by using tilted current method. The PDR using tilted current method is about three times higher than the PDR using horizontal current method, which means the tilted current method is more efficient to detect the axial crack than horizontal current method. The verification of this method through experimental measurement will be researched as a future work.

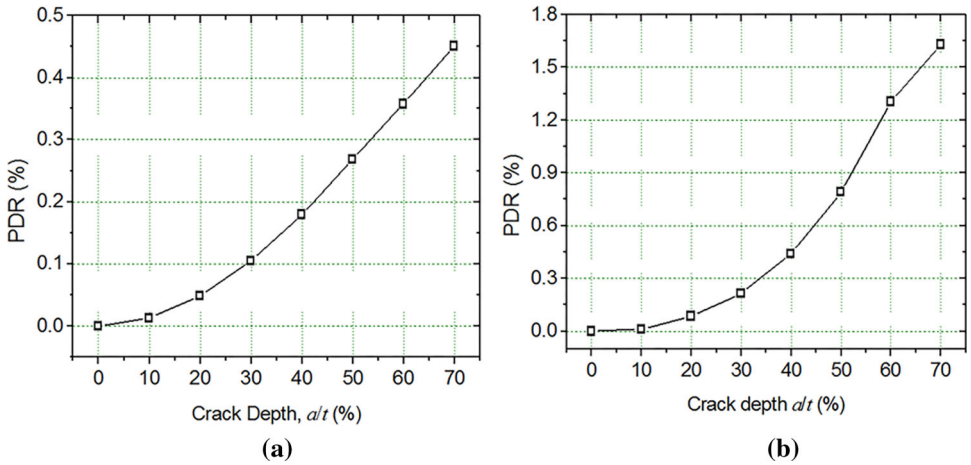


**Fig. 19** Simulated PDR of the stainless steel pipe mockup including axial crack with **a** horizontal current method by using existing ESAP-DCPD and **b** tilted current method

## 4 Conclusion

The Equi-potential Switching Array Probe Direct Current Potential Drop (ESAP-DCPD) system has been developed to monitor circumferential crack that may arise from environment-assisted cracking at piping weldment. In this paper, signal validation of the developed ESAP-DCPD has been made successfully with a good agreement among theoretical analysis, finite element analysis (FEA) and experimental measurement by using an ASTM standard center cracked tension specimen within 1.5 % error. In order to improve the ESAP-DCPD signal quality, optimal configurations of probes, current lead wires and reference signal location were determined through verified FEA. 1 A applied primary current and 0.15 A secondary current for equipotential were sent through piping weldment having an outer diameter of 335 mm and a wall thickness of 38 mm. An optimal separation of two current lead wire arrays was found to be 10 cm with 5 cm separation of measuring probes for the geometry of piping weldment. The optimal number of probe wires in each array was decided to be 12 over the circumference of the piping weld with equal spacing for real size pipe. By using optimal configuration of array probes, cracks with a depth over 10 % of pipe wall thickness could be detected through FEA analysis with adequate confidence. For noise reduction during the measurement, optimized number of power line cycles and delay time, respectively, were determined as 20 and 15 s from sensitivity study.

A dissimilar metal weld (DMW) pipe mockup containing four separate circumferential cracks with a maximum depth of 20 % of pipe wall thickness was instrumented with ESAP-DCPD in optimal conditions predicted by FEA. Through the measurements, it is not possible to detect the 20 % a/t circumferential cracks on weldments by using ESAP-DCPD. It was caused by non-uniform geometry of weldments along the circumference of pipe. Instead of DMW pipe, stainless steel pipe including four notches which are deeper than 20 % of pipe wall thickness was monitored. As a result, the notches with a depth over 40 % of thickness were detected with 1.94 % error with FEA. The reproducibility of the 40 % detectability threshold of ESAP-DCPD was confirmed by a round-robin test at three laboratories.

**Acknowledgments** This work was financially supported by the Korea Institute of Energy Technology Evaluation and Planning (KETEP), as an energy R&D funding organization of the Ministry of Trade, Industry and Energy (MOTIE). The authors gratefully acknowledge Dr. Kyung-Ha Ryu for establishing the basis of ESAP-DCPD system, and the Korea Plant Service & Engineering Co., Ltd., for providing the cracked pipe mockup. We express our sincere thanks to researchers at the Nuclear Innovative Materials laboratory at the Ulsan National Institute of Science and Technology and the Nuclear and High Temperature Materials laboratory at the Korea Advanced Institute of Science and Technology for their support and participation on the round-robin tests.

## References

1. ASME: Inservice Inspection of Nuclear Power Plant Components. ASME Boiler & Pressure Vessel Code Section XI (1992)
2. EPRI: Materials Reliability Program: Alloy 82/182 Pipe Butt Weld Safety Assessment for US PWR Plant Design. MRP-113NP. EPRI, Palo Alto, CA (2004)
3. EPRI: Materials Reliability Program: Primary System Piping Butt Weld Inspection and Evaluation Guidelines. MRP-139. EPRI, Palo Alto, CA (2005)
4. KINS: Technical Report on the Management Methods of Dissimilar Metal Welds Aging in NPPs. KINS/RR-640 (2009)
5. Rao, K.R.: Companion Guide to the ASME Boiler & Pressure Vessel Code. Criteria and Commentary on Select Aspects of the Boiler & Pressure Vessel and Piping Codes, vol. 3, 2nd edn (2006)
6. Meyer, R.M., Coble, J., Ramuhalli, P., Bond, L.J.: Advanced Instrumentation, Information, and Control System Technologies: Nondestructive Examination Technologies -FY11 Report. Pacific Northwest National Laboratory (2011)
7. Andersson, M., Persson, C., Melin, S.: Experimental and numerical investigation of crack closure measurements with electrical potential drop technique. Int. J. Fatique **28**, 1059–1068 (2006)
8. Meriaux, J., Fouvry, S., Kubiak, K.J., Deyber, S.: Characterization of crack nucleation in TA6V under fretting-fatigue loading using the potential drop technique. Int. J. Fatique **32**, 1658–1668 (2010)

9. Hofstoetter, P., Keller, H.P.: Application of the potential drop method for inservice monitoring of indications for crack initiation or crack propagation fundamental principles and practical application. In: Transactions, SMiRT 16, Washington DC, pp. 1–8 (2001)
10. Hofstotter, P., Keller, H.P., Trobitz, M., Walkmann, M.: In-service monitoring and fractographic inspection of ultrasonic indications on a feed water suction pipe of the Gundremmingen nuclear power plant. Nucl. Eng. Des. **206**, 279–289 (2001)
11. Oppermann, W., Hofstotter, P., Keller, H.P.: Long-term installations of the DC-potential drop method in four nuclear power plants and the accuracies thereby obtained for monitoring of crack initiation and crack growth. Nucl. Eng. Des. **174**, 287–292 (1997)
12. Oppermann, W., Keller, H.P.: An improved potential drop method for measuring and monitoring defects in metallic structures. Nucl. Eng. Des. **144**, 171–175 (1993)
13. Ryu, K.H., Hwang, I.S., Kim, J.H.: Development of wall thinning screening system and its application to a commercial nuclear power plant. Nucl. Eng. Des. **265**, 591–598 (2013)
14. Andresen, P.L.: IGSCC Crack Propagation Rate Measurement in BWR Environments. Executive summary of a Round Robin study; Project SKI-95118. GE Corporate Research and Development (1998)
15. Sposito, G.: Advances in Potential Drop Techniques for Nondestructive Testing. Imperial College, London (2009)
16. Ryu, K.H.: Development of Piping Wall Thinning Screening Technique Based on Equipotential Switching Driect Current Potential Drop Method. Seoul National University, Seoul (2010)
17. Rangel, J.C.F.: Pipe Wall Damage Morphology Measurement Methodology Development for Flow Assisted Corrosion Evaluation. Massachusetts Institute of Technology, Cambridge, MA (1999)
18. Ryu, K.H., Hwang, I.S., Lee, N.Y., Oh, Y.J., Kim, J.H., Park, J.H., Sohn, C.H.: Screening method for piping wall loss by flow accelerated corrosion. Nucl. Eng. Des. **238**, 3263–3268 (2008)
19. Ryu, K.H., Lee, T.H., Kim, J.H., Hwang, I.S., Lee, N.Y., Kim, J.H., Park, J.H., Sohn, C.H.: Online monitoring method using equipotential switching direct current potential drop for piping wall loss by flow accelerated corrosion. Nucl. Eng. Des. **240**, 468–472 (2010)
20. Doremus, L., Nadot, Y., Henaff, G., Mary, C., Pierret, S.: Calibration of the potential drop method for monitoring small crack growth from surface anomalies - Crack front marking technique and finite element simulations. Int. J. Fatigue **70**, 178–185 (2015)
21. Gandossi, L., Summers, S.A., Taylor, N.G., Hurst, R.C., Hulm, B.J., Parker, J.D.: The potential drop method for monitoring crack growth in real components subjected to combined fatigue and creep conditions: application of FE techniques for deriving calibration curves. Int. J. Pres. Ves. Pip. **78**, 881–891 (2001)
22. Chen, W.H., Chen, J.S., Fang, H.L.: A theoretical procedure for detection of simulated cracks in a pipe by the direct current-potential drop technique. Nucl. Eng. Des. **216**, 203–211 (2002)
23. Aronson, G.H., Ritchie, R.O.: Optimization of the electrical potential technique for crack growth monitoring in compact test pieces using finite element analysis. J. Test. Eval. **7**(4), 208–215 (1979)
24. Lee, J.H.: The influence of distance between current supply points on potential drop in DCPD. J. Korean Soc. Nondestruct. Test. **29**(2), 104–107 (2009)
25. Sato, Y., Atsumi, T., Shoji, T.: Application of induced current potential drop technique for measurements of cracks on internal wall of tube-shaped specimens. NDT&E Int. **40**, 497–504 (2007)
26. Lu, Y.: Potential Drop and Eddy Current Nondestructive Evaluation Problems. Iowa State University, Ames, IA (2012)
27. Lu, Y., Bowler, J.R., Zhang, C., Bowler, N.: Edge effects in four point direct current potential drop measurement. In: AIP Conference, Chicago. American Institute of Physics, pp. 271–278 (2008)
28. ASTM: Standard test method for measurement of fatigue crack growth rates. ASTM E647–08. West Conshohocken (PA) (2008)
29. Ho, C.Y., Chu, T.K.: Electrical resistivity and thermal conductivity of nine selected AISI stainless steels, Purdue University Technical Report, CINDAS Report No. 45. American Iron and Steel Institute (1977)